Journal of Luminescence 129 (2009) 1664–1668

Contents lists available at ScienceDirect

Journal of Luminescence

journal homepage: www.elsevier.com/locate/jlumin

Red, green, and blue lanthanum phosphate phosphors obtained via surfactant-controlled hydrothermal synthesis

Paulo C. de Sousa Filho, Osvaldo A. Serra *

Laboratório de Terras Raras, Departamento de Química, Faculdade de Filosofia, Ciências e Letras de Ribeirão Preto, Universidade de São Paulo, Brazil

ARTICLE INFO

Available online 8 May 2009

Keywords:
Luminescence
Phosphates
Hydrothermal
Europium
Terbium
Thulium

ABSTRACT

A new solution route for the obtainment of highly pure luminescent rare-earth orthophosphates in hydrothermal conditions was developed. By starting from soluble precursors (lanthanide tripolyphosphato complexes, i.e. with $P_3O_{10}^{5-}$ as a complexing agent and as an orthophosphate source) and by applying surfactants in a water/toluene medium, the precipitations are confined to reverse micelle structures, thus yielding nanosized and homogeneous orthophosphates. The method was employed to obtain lanthanide-activated lanthanum phosphates, which can be applied as red ($LaPO_4$:Eu^{3+}), green ($LaPO_4$:Ce^{3+},Tb^{3+}) and blue ($LaPO_4$:Tm^{3+}) phosphors. The produced materials were analyzed by powder X-ray diffractometry, scanning electron microscopy, infrared spectroscopy and luminescence spectroscopy (emission, excitation, lifetimes and chromaticity coordinates).

1. Introduction

Inorganic luminescent materials are nowadays widely employed in many quotidian devices and, for this, studies on their obtainment, spectroscopic behaviour and applications have been remarkable [1,2]. In particular, rare-earth orthophosphates ($REPO_4$) are a very interesting class of host lattices for activator ions due to their physico-chemical inercy (high insolubility, stability against high temperatures or against high energy excitations), thus providing durable phosphors [3]. Moreover, these materials can present high excitabilities in the vacuum ultraviolet region (VUV, at ~170 nm), which enables them an applicability in plasma display panels (PDPs) and in new generation fluorescent lamps (without mercury) [4,5]. The luminescent properties of rare-earth phosphates can be conferred by the presence of lanthanide(III) ions as activators due to their intense and narrow emission bands arising from *f*–*f* transitions, which are proper for the generation of individual colours in multiphosphor devices [6–8]. So, the red $^5D_0 \rightarrow {}^7F_2$ (~610 nm), green $^5D_4 \rightarrow {}^7F_5$ (~545 nm) and blue $^1D_2 \rightarrow {}^3F_4$ (~450 nm) emissions of Eu^{3+}, Tb^{3+} and Tm^{3+}, respectively, can be used for the design of novel phosphors. Thus, $LaPO_4$:Eu^{3+}, $LaPO_4$:Ce^{3+},Tb^{3+} and $LaPO_4$:Tm^{3+} can be considered as very promising examples of luminescent materials [9]. Specially, thulium(III)-activated lanthanum phosphate is a strong candidate for applications in PDPs, since it is one of the few examples of quite stable blue phosphors with high emission colour purity [10]. However, the applicability of these phosphates as phosphors is limited by their light output, quantum yield and emission profile, so their synthesis might allow a fine control of their morphology, purity and stoichiometry, which directly affects these properties. In this way, solution-based methods are preferred and widely employed for the synthesis of these materials [11–15], once they allow a homogeneous distribution of the precursors in the initial mixture and allow the development of bottom-up approaches for the obtainment of nanostructures. Moreover, they are of low cost, simple, secure, relatively fast and of low energetic consumption. This work reports on a new type of hydrothermal synthesis for nanosized and highly pure rare-earth orthophosphates.

Here, we present a reverse micelle approach for the control of the morphological properties of the solids, based on the action of surfactants in mixtures of aqueous and non-aqueous media, thus confining the precipitations in small reactional volumes (and stabilizing the particles against growth and redissolution). The homogeneity of the starting solution is ensured by utilizing soluble lanthanide tripolyphosphato complexes as precursors for the solids [15,16].

2. Experimental

Rare-earth nitrate solutions (0.10 mol L^{-1}) were prepared through dissolution of the previously calcinated oxides (La_2O_3, Eu_2O_3, Tb_4O_7 and Tm_2O_3 99.99% Rhône-Poulenc/Rhodia, and

* Correspondence to: Laboratorio de Terras Raras, Departamento de Química, Faculdade de Filosofia, Ciências e Letras de Ribeirão Preto, Universidade de São Paulo. Av. Bandeirantes, 3900, CEP 14040-901, Ribeirão Preto, SP, Brazil.
Tel.: +55 16 3602 4376, +55 16 3602 3746.
E-mail address: osaserra@usp.br (O.A. Serra).

0022-2313/$ - see front matter © 2009 Elsevier B.V. All rights reserved.
doi:10.1016/j.jlumin.2009.04.075

CeO_2 99.995% Aldrich) in concentrated nitric acid. Sodium tripolyphosphate hexahydrate ~99% ($Na_5P_3O_{10}\cdot 6H_2O$, purified through recrystallization from the Acros-85%) was utilized in all processes. For the synthesis of the lanthanum phosphates, appropriated volumes of 0.10 mol L^{-1} $RE(NO_3)_3$ solutions (RE^{3+} = $(La_{0.99}Eu_{0.01})^{3+}$, $(La_{0.55}Ce_{0.30}Tb_{0.15})^{3+}$ or $(La_{0.99}Tm_{0.01})^{3+}$) were mixed with equimolar quantities of $Na_5P_3O_{10}.6H_2O$ (RE^{3+}:-$P_3O_{10}^{5-}$ = 1:1) and the pH of this solution was adjusted to ~3 with addition of 1 mol L^{-1} nitric acid. Sodium dodecylsulfate (SDS, 90% Synth) was added in a relation RE^{3+}:SDS = 1:5. The yellowish and limpid aqueous solution is diluted to the double of its volume and is then dispersed in toluene (water:toluene = 1:2) yielding a white emulsion, which is heated in a hermetically closed tube in an oil bath at 190±10 °C (10–15 atm) for 4 h under intense stirring. The obtained powders were centrifuged and washed with fresh water, ethanol and ethyl ether, and stored in a desicator over silica. For the elimination of hydration waters, the powders were post-annealed at 900 °C for 2 h.

The emission and excitation spectra were acquired at room temperature on a Jobin-Yvon SPEX Triax 550 FluoroLog 3 spectrofluorometer, equipped with 450 W xenon lamp. All the spectra were corrected, with the software apparatus, for the lamp intensity and photomultiplier sensitivity at the monitored wavelengths. Luminescence lifetime measurements were carried out with a SPEX 1934D phosphorimeter with a pulsed xenon lamp. The crystallinity of the materials was evaluated by powder X-ray diffraction (XRD) in a Siemens D5005 diffractometer. The morphological analyses were performed in a Zeiss EVO 50 scanning electron microscope (SEM). Fourier transform infrared spectroscopy (FT-IR), carried out in an ABB Bomen FTLA2000-100 spectrometer using KBr pellets, was also applied for the characterizations.

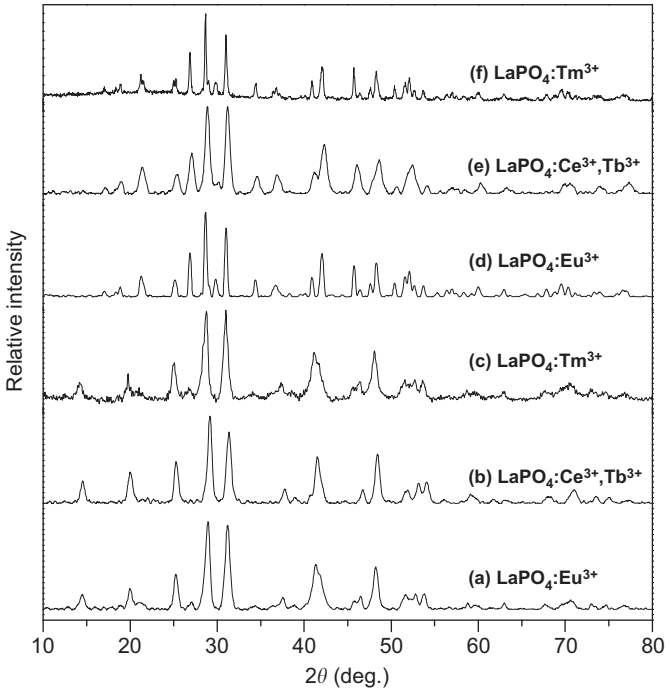

Fig. 1. Powder X-ray diffractograms of hydrated (a–c) and calcinated (d–f) lanthanum phosphates.

3. Results and discussion

In all cases, the powder XRD analysis (Fig. 1) evidenced the obtainment of hydrated orthophosphates with hexagonal Rhabdophane-type structure ($REPO_4\cdot xH_2O$, RE = La, Ce, Nd and $0.5<x<1$), whose spatial groups are $P6_222$ (D_6^4) and $P3_121$ (D_3^4) [17]. After the post-annealing processes, the phosphates lose their hydration waters and are converted into Monazite-type orthophosphates (with monoclinic $P2_1/m$ structure [17]). The average crystallite sizes estimated by the Scherrer equation are ~15–20 nm for hydrated and ~40 nm for the calcinated phosphates. The increase in crystallite size with the calcination is due to the coalescence of particles at high temperatures, as already observed for other phosphates [16]. The purity of the obtained powders is also attested by the FT-IR spectra (not shown), in which only PO_4^{3-} bands (besides, bands related to lattice waters in hydrated phosphates) are observed, with absorption profiles in agreement with those reported in the literature [3,18,19]. Bands ascribed to hydrogenphosphates or polyphosphates, which are possible contaminants, were not observed in any cases.

SEM images (Fig. 2) attest for the obtainment of homogeneous solids, which occur as micrometric aggregates (0.5–3.0 μm) of nanosized structures. The particles composing these microaggregates have a spherical shape and sizes ranging from ~20 to 100 nm. These results are in agreement with the expected for the reverse micelle approach applied to the synthesis, that yields spherical and uniform nanoparticles which, however, with the isolation of the solid from the mother solution, agglomerate in larger structures. The post-annealing process, which is necessary for an adequate evaluation of the luminescent behaviour of these materials, causes a gathering of particles and partial loss of their nanostructure character.

The photoluminescent properties under UV excitation of the obtained phosphates (after the thermal treatments) are presented in Fig. 3. The excitation spectrum of $LaPO_4:Eu^{3+}$ (Fig. 3a) presents a broad and intense band with maximum at ~280 nm, related to a ligand–metal charge transfer between PO_4^{3-} groups and Eu^{3+} ions.

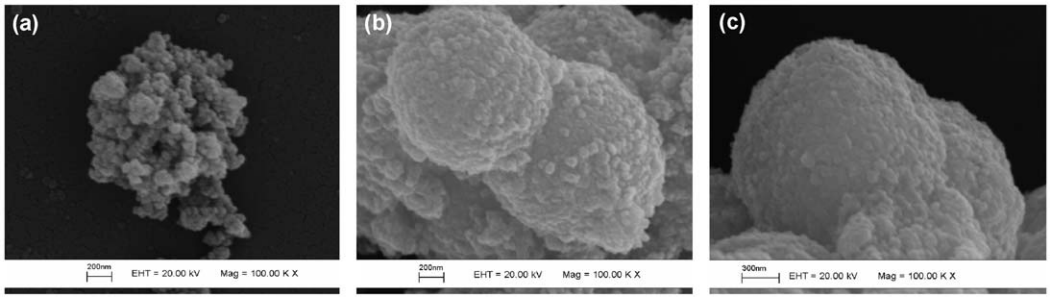

Fig. 2. Scanning electron micrographs of hydrated lanthanum phosphates: (a) $LaPO_4:Eu^{3+}$, (b) $LaPO_4:Ce^{3+},Tb^{3+}$, and (c) $LaPO_4:Tm^{3+}$.

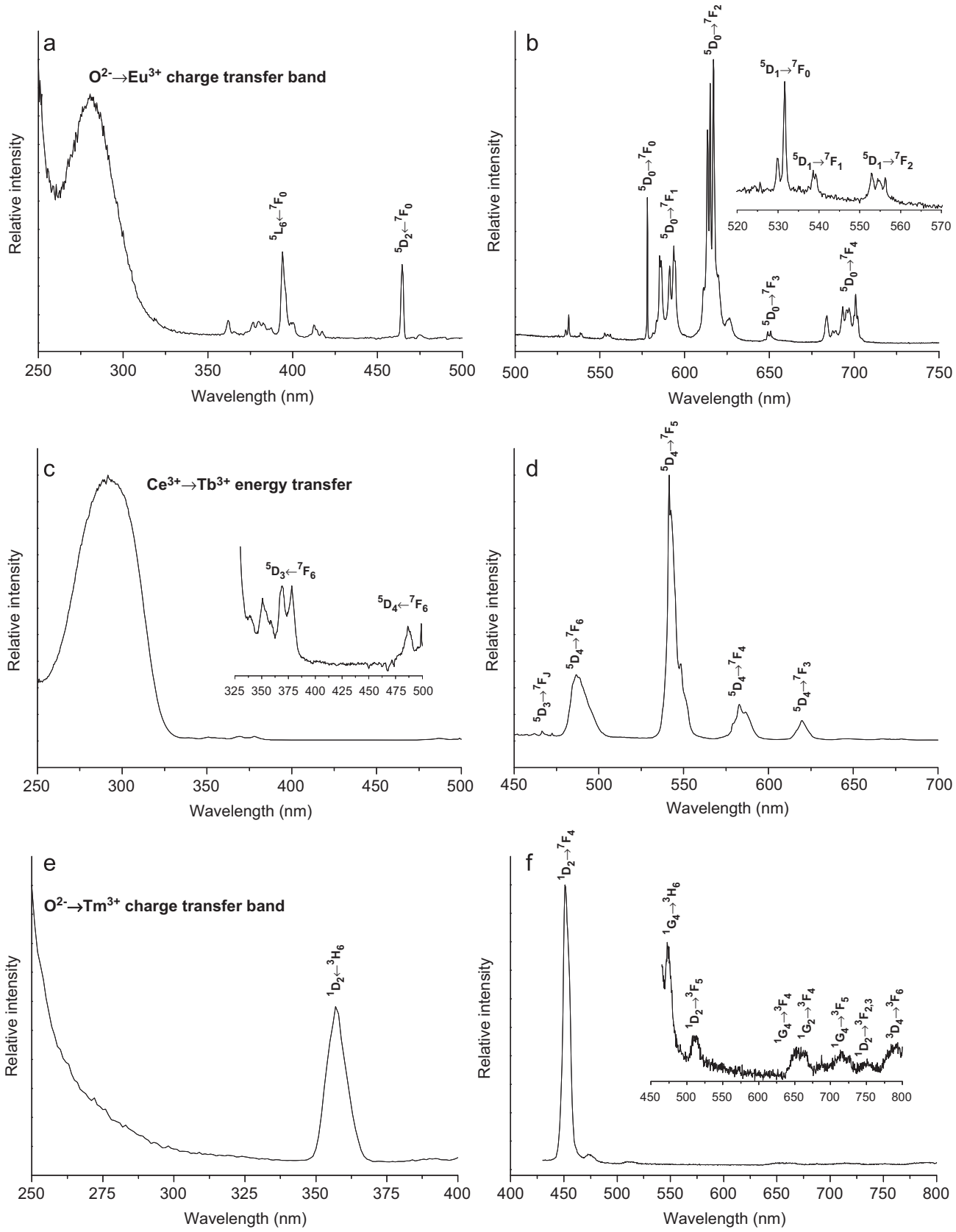

Fig. 3. Excitation and emission spectra at 298 K of: (a, b) $LaPO_4:Eu^{3+}$ ($\lambda_{em} = 615$ nm; $\lambda_{ex} = 394$ nm), (c, d) $LaPO_4:Ce^{3+},Tb^{3+}$ ($\lambda_{em} = 542$ nm, $\lambda_{ex} = 290$ nm) and (e, f) $LaPO_4:Tm^{3+}$ ($\lambda_{em} = 451$ nm, $\lambda_{ex} = 358$ nm).

The weaker Eu^{3+} intraconfigurational f–f transitions (^5H_J,^5L_J,$^5D_J \leftarrow {}^7F_0$) are also observable in the excitation spectrum, with the two main peaks ascribed to the $^5L_6 \leftarrow {}^7F_0$ transition (at 394 nm) and to the hypersensitive $^5D_2 \leftarrow {}^7F_0$ transition ($\Delta J = 2$) at 464 nm. The emission spectrum of $LaPO_4$:Eu^{3+} (Fig. 3b) displays the characteristic $^5D_0 \rightarrow {}^7F_J$ transitions of Eu^{3+}. Emissions from the $^5D_1$ state are also observed, accounting for a low rate of multiphonon deactivation of the upper excited states. The $^5D_0 \rightarrow {}^7F_0$ transition occurs as a unique, sharp and intense line (~3 Å width), indicating the occupation of a site of low symmetry (C_s) [6,8], in agreement with the monoclinic structure; this also attests for the high purity of this orthophosphate. The predominance of the hypersensitive $^5D_0 \rightarrow {}^7F_2$ transition in the emission spectrum (which is not often reported for Eu^{3+}-activated lanthanum orthophosphates [3,12,14–16]) is determinant for the applicability of this material, once only in this way a high emission red colour purity is achieved. In the present case, the low contributions of the orange $^5D_0 \rightarrow {}^7F_1$ emissions and the high intensity of the $^5D_0 \rightarrow {}^7F_2$ emission results in high colour purities: CIE 1931 chromaticity coordinates $x \approx 0.66$ and $y \approx 0.34$ (Table 1, Fig. 4) that are acceptable for many optical applications [2,4,16]. The luminescence persistence determined for this phosphate (by fitting the emission decay by a first-order exponential curve) was 1.62 ms ($^5D_0$ level) (Table 1).

In the $LaPO_4$:Ce^{3+},Tb^{3+} excitation spectrum (Fig. 3c), some f–f absorptions of Tb^{3+} ($^5D_3 \leftarrow {}^7F_6$ and $^5D_4 \leftarrow {}^7F_6$) are poorly observed, and the allowed $5d \leftarrow 4f$ absorption of Ce^{3+} at ~290 nm, which is followed by $Ce^{3+} \rightarrow Tb^{3+}$ energy transfer [6], is predominant. The emission spectrum of this phosphate (Fig. 3d) displays the $^5D_4 \rightarrow {}^7F_J$ ($J = 6, 5, 4, 3$) Tb^{3+} transitions, besides the weak emissions of $^5D_4 \rightarrow {}^7F_3$ transition at ~460 nm. Although the emission bands are relatively broad (due to the high number of components of Tb^{3+} manifolds and to the high concentration of activator ions), the predominance of the $^5D_4 \rightarrow {}^7F_5$ transition at ~542 nm confers a high green colour purity for this compound ($x \approx 0.25$ and $y \approx 0.57$) (Table 1, Fig. 4), which is a well-established commercial phosphor [1,2,6]. The $^5D_4$ luminescence lifetime of Tb^{3+} observed in this phosphate was 4.11 ms. One has to observe, however, that the presence of Ce^{3+} (that acts as a sensitizer for UV excitation) in $LaPO_4$ host actually traps terbium(III) luminescence for VUV excitation [5], so this phosphor still must be adapted for this new kind of application.

The excitation spectrum of $LaPO_4$:Tm^{3+} (Fig. 3e) presents the only intraconfigurational absorption of Tm^{3+} in the near-UV region, relative to the $^1D_2 \leftarrow {}^3H_6$ transition at ~358 nm, besides an intense and broad excitation band with maximum energies greater than 40,000 cm^{-1}, which can be ascribed to $O^{2-} \rightarrow Tm^{3+}$ charge transfer band. In its emission spectrum under excitation on the $^1D_2$ level (Fig. 3f), this phosphate presents a dominant emission at ~451 nm, as an outcome of the radiative $^1D_2 \rightarrow {}^3F_4$ Tm^{3+} transition, thus resulting in a relatively low Stokes shift of ~5760 cm^{-1}. The other Tm^{3+} f–f emissions (arising from $^1D_2$, $^1G_4$, and $^3H_4$ levels) are very weak and do not have a significant contribution to the emission spectrum. The occurrence of only one transition with appreciable intensity confers a very high-emission blue colour purity for this phosphate ($x \approx 0.15$ and $y \approx 0.03$) (Table 1, Fig. 4), which is one of the major features that make $LaPO_4$:Tm^{3+} very promising as a blue phosphor. The luminescence persistence determined for the emitter state of Tm^{3+} ($^1D_2$) is of ~50 μs, a very short value in comparison with the other phosphates. This material may present a low degree of degradation, once both the activator (trivalent thulium) and the host lattice are quite stable to the operation conditions. However, high energy excitations (VUV, for example) on $LaPO_4$:Tm^{3+} result in a relatively high UV output, due to emissions from the upper excited states (^3P_J, ^1I_J, $^1D_2$) to the $^3H_6$ ground state [10], which does not compromises, notwithstanding, the chromaticity of the compound.

Table 1
Luminescence lifetimes and chromaticity coordinates (CIE 1931) [20] of the obtained phosphates.

	τ (ms)	Chromaticity coordinates	
		x	y
$LaPO_4$:Eu^{3+}	1.62 ($^5D_0$)	0.66	0.34
$LaPO_4$:Ce^{3+},Tb^{3+}	4.11 ($^5D_4$)	0.25	0.57
$LaPO_4$:Tm^{3+}	0.05 ($^1D_2$)	0.15	0.03

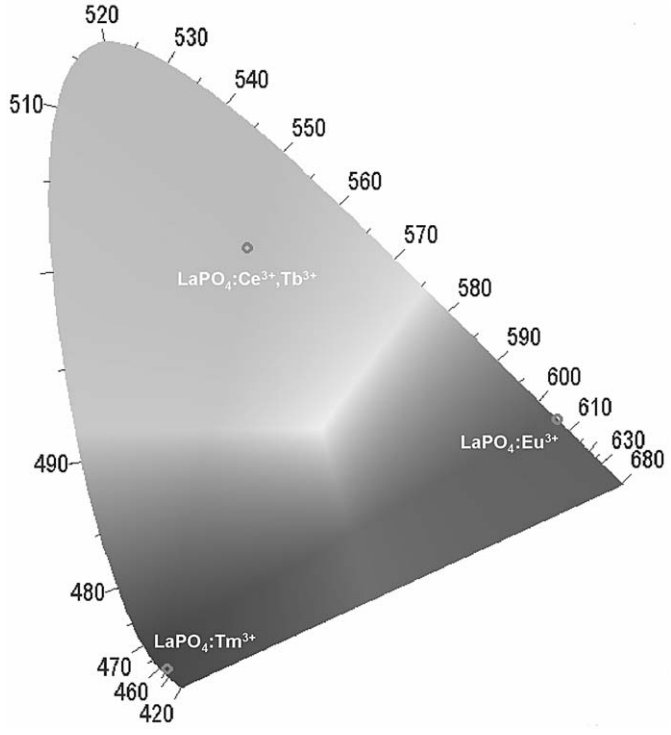

Fig. 4. Positioning of the synthesized lanthanum phosphate emissions in the chromaticity diagram [20].

4. Conclusion

A new solution route (hydrothermal method) comprising a reverse micelle approach for the synthesis of rare-earth orthophosphate phosphors was developed. In a relatively simple and fast way (whose only inconvenient is the generation of organic solvent residues), highly pure (without contaminations of hydrogenphosphates or polyphosphates) and homogeneous lanthanide-activated lanthanum phosphates were synthesized, by starting from rare-earth nitrate, sodium tripolyphosphate and SDS aqueous solutions dispersed in toluene. The obtained powders were composed by micrometric agglomerates of nanosized (20–100 nm) structures of Rhabdophane-type orthophosphates. After the elimination of the hydration waters (thus producing Monazite-type orthophosphates), the materials present very attractive luminescent properties for the generation of the three primary colours, due to the red, green and blue emissions of $LaPO_4$:Eu^{3+}, $LaPO_4$:Ce^{3+},Tb^{3+} and $LaPO_4$:Tm^{3+}, respectively.

Particularly, $LaPO_4:Eu^{3+}$ presents a luminescent behaviour very different from the often reported, and $LaPO_4:Tm^{3+}$ can be pointed as a very promising blue phosphor due to its high stability and alluring photophysical characteristics. Moreover, the luminescent properties of these compounds open the possibility of developing a tri-colour phosphor containing only the quite stable lanthanide-activated lanthanum phosphates for applications in PDPs and lamps without mercury.

Acknowledgements

The authors thank Dr. R.F. Silva for helpful discussion, and the Brazilian agencies CAPES, CNPq and FAPESP for financial support.

References

[1] C. Feldman, T. Jüstel, C. Ronda, P. Schmidt, Adv. Funct. Mater. 13 (2003) 511.
[2] T. Jüstel, H. Nikol, C. Ronda, Angew. Chem. Int. Ed. 37 (1998) 3084.
[3] L. Niinistö, M. Leskelä, in: K.A. Gschneidner Jr., L. Eyring (Eds.), Handbook on the Physics and Chemistry of Rare Earths, Elsevier, Amsterdam, 1987 (Chapter 59).
[4] D.C. Tuan, R. Olazcuaga, F. Guillen, A. Garcia, B. Moine, C. Fouassier, J. Phys. IV 123 (2005) 259.
[5] B. Moine, G. Bizarri, Opt. Mater. 28 (2006) 58.
[6] G. Blasse, B.C. Grabmaier, Luminescent Materials, Springer, Berlin, 1994 (Chapters 2–6).
[7] P. Porcher, in: R. Saez, P.A. Caro (Eds.), Rare Earths, Editorial Complutense, Madrid, 1999 (Chapter 3).
[8] J.-C.G. Bünzli, in: J.-C.G. Bünzli, G.R. Choppin (Eds.), Lanthanide Probes in Life, Chemical and Earth Sciences, Elsevier, Amsterdam, 1989 (Chapter 7).
[9] R.P. Rao, D.J. Devine, J. Lumin. 87–89 (2000) 1260.
[10] R.P. Rao, J. Lumin. 113 (2005) 271.
[11] S.S. Brown, H.-J. Im, A.J. Rondinone, S. Dai, J. Colloid Interface Sci. 292 (2005) 127.
[12] Y.-P. Fang, A.-W. Xu, R.-Q. Song, H.-X. Zhang, L.-P. You, J.C. You, H.-Q. Liu, J. Am. Chem. Soc. 125 (2003) 16025.
[13] K. Rajesh, P. Shajesh, O. Seidel, P. Mukundan, K.G.K. Warrier, Adv. Funct. Mater. 17 (2007) 1682.
[14] K. Riwotzki, H. Meyssamy, A. Kornowski, M. Haase, J. Phys. Chem. B 104 (2000) 2824.
[15] V. Buissette, M. Moreau, T. Gacoin, J.-P. Boilot, J.-Y. Chane-Ching, T. Le Mercier, Chem. Mater. 16 (2004) 3767.
[16] P.C. de Sousa Filho, O.A. Serra, J. Fluoresc. 18 (2008) 329.
[17] R.C.L. Mooney, Acta Crystallogr. 3 (1950) 337.
[18] R. Kijkowska, E. Cholewka, B. Duszak, J. Mater. Sci. 38 (2003) 223.
[19] A. Hezel, S.D. Ross, Spectrochim. Acta 22 (1966) 1949.
[20] P.A. Santa-Cruz, F.S. Teles, Spectra Lux Software v.2.0, Ponto Quântico Nanodispositivos/RENAMI (Brazil), 2003.